Final version published at:

European Journal of Medicinal Chemistry
Volume 176, 15 August 2019, Pages 105-116

DOI: 10.1016/j.ejmech.2019.05.016

https://www.sciencedirect.com/science/article/pii/S0223523419304258?via%3Dihub

Sequence modification of heptapeptide selected by phage display as homing device for HT-29 colon cancer cells to improve the anti-tumour activity of drug delivery systems

Krisztina Kiss[a,b], Beáta Biri-Kovács[a,b], Rita Szabó[a], Ivan Ranđelović[c], Kata Nóra Enyedi[a,b], Gitta Schlosser[a,b], Ádám Orosz[d], Bence Kapuvári[c], József Tóvári[c], Gábor Mező[a,b*]

[a] MTA-ELTE Research Group of Peptide Chemistry, Hungarian Academy of Sciences, Eötvös L. University, 1117 Budapest, Hungary

[b] Institute of Chemistry, Eötvös L. University, 1117 Budapest, Hungary

[c] Department of Experimental Pharmacology, National Institute of Oncology, 1122, Budapest, Hungary

[d] Institute of Biophysics and Radiation Biology, Semmelweis University, 1444, Budapest, Hungary

[*] Corresponding author, 1117 Budapest, Pázmány Péter sétány 1/A, Hungary; gmezo@elte.hu

Abstract

Development of peptide-based conjugates for targeted tumour therapy is a current research topic providing new possibilities in cancer treatment. In this study, VHLGYAT heptapeptide selected by phage display technique for HT-29 human colon cancer was investigated as homing peptide for drug delivery. Daunomycin was conjugated to the *N*-terminus of the peptide directly or through Cathepsin B cleavable spacers. Conjugates showed moderate *in vitro* cytostatic effect. Therefore, sequence modifications were performed by Ala-scan and positional scanning resulting in conjugates with much higher bioactivity. Conjugates in which Gly was replaced by amino acids with bulky apolaric side chains provided the best efficacy. The influence of the cellular uptake, stability and drug release on the anti-tumour activity was investigated. It was found that mainly the difference in the cellular uptake of the conjugates generated the distinct effect on cell viability. One of the most efficient conjugate Dau=Aoa-LRRY-VHLFYAT-NH_2 showed tumour growth inhibition on orthotopically developed HT-29 colon cancer in mice with negligible toxic side effect compared to the free drug. We also indicate that this sequence is not specific to HT-29 cells, but it has a remarkable effect on many other cancer cells. Nevertheless, the Phe-containing conjugate was more active in all cases compared to the conjugate with the parent sequence. The literature data suggested that this sequence is highly overlapped with peptides that recognize Hsp70 membrane bound protein overexpressed in many types of tumours.

Keywords

drug delivery system, phage display, targeted cancer therapy, daunomycin, small molecule drug conjugate, drug release

1. Introduction

Colon cancer has become the third most commonly diagnosed cancer and the fourth leading cause of death related to cancer in the world [1, 2]. Besides the conventional treatments of colon cancer (surgery, radiation therapy and chemotherapy), targeted therapy is one of the main therapeutic approaches that might have significant role in the future [3]. The most remarkable advantages of targeted cancer therapy over the conventional chemotherapy are the specificity towards cancer cells while sparing toxicity to off-target cells and the avoidance of multi-drug resistance (MDR) that are the major obstacles in cancer chemotherapy [4]. The concept of selective drug targeting is based on the high expression of certain cell surface components on tumours or the tumour neovasculature [5]. The two main groups of targeting moieties are antibodies [6] and small homing peptides like peptide hormones [7, 8]. Peptides having high binding affinities to tumour selective or overexpressed receptors in cancer cells are useful because of their simple structure, low immunogenicity and easy, cost-effective chemical synthesis compared to antibody drug conjugates (ADCs). In the last decades, many developments have been done in the field of peptide based small molecule drug conjugates (SMDCs), particularly for cancer therapy [9]. However, the efficacy of these conjugates was studied rather individually on cancer cells. Nevertheless, the number of receptors in cancer cells is limited, therefore, the elevation of the drug conjugate concentration alone might not enhance the anti-tumour effect. To overcome this drawback, the combination of SMDCs could provide increased biological activity [10]. Therefore, the search of new tumour homing peptides is a hot topic in targeted cancer therapy [11]. One of the approach often used to explore new peptides is a technique belonging to *in vitro* evolution methods: phage display is a useful tool to identify tumour specific peptides that can be used efficiently for anti-cancer drug targeting [12].

Zhang and his co-workers selected HT-29 human colon cancer specific heptapeptides by phage display technology [13]. In the *in vitro* panning experiment, a 7-mer phage-display peptide library containing 10^{11} pfu was used (*ca.* 100 clones belong to one peptide sequence). After three rounds of panning using colon cancer cell lines and two rounds of subtractive screening, the peptide sequences of 50 randomly picked phage clones were analysed by cell – enzyme-linked immunosorbent assay. The heptapeptide VHLGYAT was found as the most selective peptide to HT-29 colon cancer cell line. It has to be noted that the receptor recognized by this peptide was not identified.

In our previous studies, gonadotropin-releasing hormone peptide derivative – drug conjugates were applied as drug delivery systems (DDS) for colon cancer treatment [14]. In *in vitro* experiments, the most efficient compounds in which daunomycin (Dau) was attached to modified lamprey GnRH-III *via* oxime linkage were Glp-His-Trp-Lys(Bu)-His-Asp-Trp-Lys(Dau=Aoa)-Pro-Gly-NH_2 and Glp-*D*-Tic-Lys(Bu)-His-Asp-Trp-Lys(Dau=Aoa)-Pro-Gly-NH_2 (where Glp is pyroglutamic acid, Bu is butyryl, Aoa is aminooxyacetyl moiety and Tic is 1,2,3,4-tetrahydroisoquinoline-3-carboxylic acid) [15, 16]. Daunomycin is attached to the side chain of Lys in position 8. This conjugate showed a pronounced cytostatic effect with a 2-3 μM IC_{50} value on HT-29 cells in MTT assay. Furthermore, the first conjugate showed higher tumour growth inhibition and lower toxic side effects on orthotopically developed HT-29 tumour bearing mice than the free Dau in maximal tolerated dose (40% inhibition instead of 30%) [17]. It is worth mentioning that the oxime linkage is stable not only in human plasma (in contrast to ester bond) but also in the presence of Cathepsin B (an overexpressed lysosomal enzyme in cancer cells that plays role in the degradation of conjugates taken up by receptor mediated pathway) or in lysosomal homogenate. Therefore, the smallest metabolite released from conjugates is the daunomycin connected to an amino acid through oxime bond (Dau=Aoa-Aaa-OH), in the case of the above mentioned conjugates, it is H-Lys(Dau=Aoa)-OH [18]. These metabolites bind to DNA as site of action, but with a bit lower efficacy than the free drug.

For the improvement of tumour growth inhibition, we planned to develop further conjugates that can be used in combination for targeted cancer therapy. For this purpose, the VHLGYAT heptapeptide selected by Zhang *et al.* for HT-29 cells was chosen as homing device [13]. In this study, first we developed three conjugates and selected the most active one for further experiments. In addition, it was suspected that by the random selection of 50 clones from the panned and screened phages, some compounds with higher affinity and/or selectivity were lost. Thus, Ala scan and positional scan procedures were used to find more active conjugates. Next to the stability studies of the conjugates under circumstances used for *in vitro* and *in vivo* experiments, their degradation in lysosomal homogenate was investigated. Finally, two conjugates were selected for *in vivo* studies. In addition, we also report here that the peptide sequence was not selective to HT-29 cancer cells that might confirm the suggested target molecules which are overexpressed on most types of tumour cells.

2. Materials and methods

2.1. Materials

N,N′-diisopropylcarbodiimide (DIC), 1,8-diazabicyclo[5.4.0]undec-7-ene (DBU), 1-hydroxybenzotriazole hydrate (HOBt), triisopropylsilane (TIS) and ninhydrin were purchased from Sigma-Aldrich Kft. (Budapest, Hungary). All other reagents and solvents (anhydrous) were obtained from VWR International Kft. (Debrecen, Hungary). Fmoc-Rink Amide MBHA resin and all amino acid derivatives used in this study were purchased from Iris Biotech GmbH (Marktredwitz, Germany). Isopropylidene protected aminooxyacetic acid derivative was prepared in our laboratory [19].

2.2. Peptide synthesis and conjugation of Dau to peptide derivatives

Peptides were prepared by solid phase peptide synthesis using the standard Fmoc/tBu procedure on Rink-Amide MBHA resin (for details, see Supporting Information Materials and methods section). After assembling the linear peptides, the isopropylidene protected aminooxyacetic acid (Aoa) was attached to their *N*-termini on the resin. The side chain unprotected peptides were cleaved from the resin as well as the removal of side chain protecting groups was made by treatment with 95% TFA, 2.5% TIS and 2.5% water (v/v/v) mixture. The yield of the purified peptide derivatives was between 45–60%. Prior to the conjugation, the isopropylidene protecting group from Aoa was removed with 1 M methoxyamine containing buffer solution as it is described in [19]. The reaction mixture was purified by RP-HPLC to separate the unprotected functionalized peptides and Dau was conjugated to the aminooxyacetylated peptides in 0.2 M NH_4OAc solution (pH 5.0) at a 10 mg/mL concentration. The conjugation ran almost quantitatively in all cases. The resulting conjugates were analysed by analytical RP-HPLC and electrospray ionization mass spectroscopy (ESI-MS). The purity of the conjugates was over 95% in all cases and no free Dau impurity was detected.

2.3. Reverse phase high performance liquid chromatography (RP-HPLC)

The crude peptides and conjugates were purified as described in [19]. Analytical RP-HPLC in case of conjugates **1-9** was performed as described in [19], for the rest of the conjugates a Macherey-Nagel Nucleosil C18 column (5 μm, 100 Å; 250×4.6 mm) (Macherey-Nagel GmbH & Co. Düren, Germany) column was used.

2.4. Mass spectrometry (MS)

Electrospray ionization (ESI)-MS analyses were carried out as detailed in [19].

LC-MS analyses were performed on a Q Exactive™ Focus, high resolution and high mass accuracy, hybrid quadrupole-orbitrap mass spectrometer (Thermo Fisher Scientific, Bremen, Germany) using on-line UHPLC coupling. UHPLC separation was performed on a Dionex 3000 UHPLC system using a Supelco Ascentis C18 column (2.1 x 150 mm, 3 μm). Linear gradient elution (0 min 2% B, 1 min 2% B, 17 min 90% B) with eluent A (0.1% HCOOH in water, v/v) and eluent B (0.1% HCOOH in acetonitrile/water, 80:20, v/v) was used at a flow rate of 0.2 mL/min at 40 °C. High resolution mass spectra were acquired in the 200–1600 *m/z* range. LC-MS data were analysed by Xcalibur™ software (Thermo Fisher Scientific) and with Origin Pro 8 (OriginLab Corp., Northampton, MA, USA).

2.5. Stability studies

To imitate the conditions used in cellular uptake studies and *in vitro* cytotoxicity assay, stability of the conjugates was measured in serum-free medium and 2.5% Fetal Bovine Serum (FBS) containing medium, respectively. Conjugates (30 μM) were incubated in the media at 37 °C, samples were taken at 0 and 3 h (in case of serum-free medium) and at 0, 3, 6 and 24 h (in case of 2.5% FBS containing medium), aliquots were quenched with acetic acid. After lyophilisation, samples were prepared for LC-MS analyses using Pierce C18 spin columns (Thermo Fisher Scientific).

The conditions of the *in vivo* studies were imitated by incubation of the conjugates in 90% human plasma derived from a healthy volunteer. The plasma stability study was carried out as can be seen in [16], except for the incubation times which were 0, 5 and 60 min.

2.6. Metabolism in lysosomal homogenate

The stability study in rat liver lysosomal homogenate is described in [16] with few exceptions: the concentration of the mixed conjugates and the rat liver lysosomal homogenate were both 0.05 μg/μL and aliquots were taken at 0, 1, 3, 6 and 24 h.

2.7. Cell culturing and *in vitro* cytostatic effect studies

HT-29 human colon adenocarcinoma cells were cultured as described in [20].

The description of the *in vitro* cytostatic effect study can be seen in [21], except for the incubation time with the conjugates that was in this case 24 h (followed by a washing step and 48 h additional incubation).

For the specificity study of the drug conjugates, the following cell lines were used: MDA-MB-231 and MCF7 (human breast cancer), 4T1 (mouse breast cancer), DU145 and PC-3 (human prostate cancer), OVCAR-3 (human ovarian cancer), Hep G2 (human liver cancer), A2058, WM983B and M24 (human melanoma), B16 (mouse melanoma), H1975, H1650 and A549 (human lung cancer), HT-29, HCT116 and WiDr (human colorectal adenocarcinoma), CT26.WT (mouse colon cancer), PANC-1 (human pancreatic cancer) which were cultured in RPMI-1640 medium, then U-87 MG (human malignant glioma) and MRC-5 (human fibroblast) which were cultured in Dulbecco's Modified Eagle's Medium (DMEM, Lonza) and PE/CA-PJ15 and PE/CA-PJ41 (human oral cancer) which were cultured in Iscove's Modified Dulbecco's Medium (IMEM) (Sigma-Aldrich). All mediums were supplemented with 10% heat-inactivated FBS (Euro Clone, Pero, Italy) (20% FBS for OVCAR-3 cell line) and with 1% penicillin/streptomycin (Sigma-Aldrich). Cell lines were obtained from ATCC, except for PE/CA-PJ15, PE/CA-PJ41 (ECACC), A2058 (kindly provided by L. A. Liotta, NCI, Bethesda, MD, USA), M24 (kind gift from B. M. Mueller, Scripps Research Institute, La Jolla, CA, USA) and WM983B (kindly provided by Meenhard Herlyn, Wistar Institute, Philadelphia, PA, USA). Cells were cultured in sterile T25 flasks with ventilation cap (Sarstedt, Nümbrecht, Germany) at 37 °C in a humidified atmosphere with 5% CO_2.

The *in vitro* cytostatic effect on these cell lines was measured using MTT assay, similarly as described above. Cells were seeded at a density of 3×10^3 - 10×10^3 cells per well (dependent on the cell line). At the end of the measurement, absorbance values of treated samples were normalized versus untreated control samples and interpolated by nonlinear regression analysis with Prism 6 software (GraphPad, La Jolla, CA, USA) to generate dose-response curves.

2.8. Cellular uptake determination by flow cytometry

For determining cellular uptake of the bioconjugates by HT-29 cells, flow cytometry was used (details can be seen in [21]), except for the incubation time with the conjugates that was 3 h.

2.9. Confocal microscopy imaging

Intracellular localization studies were conducted with a Zeiss 710 confocal microscope (Carl Zeiss Microscopy, Jena, Germany), as described in [22]. Briefly, Dau-peptide conjugates were added to a final concentration of 50 μM in RPMI medium to the cells and incubated for 90 min. For co-localization experiments, organelle specific fluorescent labels were used to stain lysosomes and mitochondria (LysoTracker Deep Red and MitoTracker Deep Red, Molecular Probes (Eugene, OR, USA)). Samples containing the Dau-peptide conjugates were excited at 488 nm while detecting the fluorescence emission between 550-600 nm. In the case of lysotracker and mitotracker, the excitation wavelength was 633 nm and detection interval was 680-730 nm. The acquired images were elaborated with ZEN lite software (Zeiss Microscopy).

2.10. *In vivo* anti-tumour effect of conjugates on orthotopical human HT-29 colon carcinoma bearing SCID mice

6–8 weeks old, immunodeficient SCID female mice (weighing 22–27 g) were used in this experiment. Tumour development and transplantation was performed by using HT-29 colon carcinoma cells (obtained from ATCC and cultured according to their standards), the procedure is detailed in [17]. The treatments started 13 days after tumour transplantation by intraperitoneal administration of the compounds dissolved in distilled water for injection (Pharmamagist Kft., Budapest, Hungary). For the treatment, 8–8 mice/group were used. One group of mice were treated with free Dau (1 mg/kg body weight) on days 13 and 20 after tumour transplantation. Groups that received conjugates (**3**) and (**13**) were treated with a dose of 10 mg/kg Dau content (36.6 and 38.3 mg/kg of each conjugate, respectively) on days 13, 16, 20, 23 and 27 after tumour transplantation. Control group was treated with solvent. The experiment was terminated on day 30 after tumour transplantation. Daunomycin group was terminated on day 23 after tumour transplantation due to significant weight loss of the animals. The mice from all groups were killed by cervical dislocation. Their tumours and livers were removed and weighed. The animals used in these studies were cared for according to the ‘Guiding Principles for the Care and Use of Animals’ based upon the Helsinki declaration, and they were approved by the local ethical committee. Permission license for breeding and performing experiments with laboratory animals: PEI/001/1738-3/2015 and PEI/001/2574–6/2015.

2.11. Immunohistochemical staining and scoring of Ki-67

Monoclonal mouse antibody against human Ki-67 (DAKO, Glostrup, Denmark) was applied. The routinely formalin-fixed tumours were dehydrated in a graded series of ethanol, infiltrated with xylene and embedded into paraffin at a temperature not exceeding 60 °C. Two micron thick sections were mounted on Superfrost slides (Thermo Shandon, Runcorn, UK) and were manually deparaffinized. To block endogenous peroxidase activity, slides were treated for 20 min at room temperature with 3% H_2O_2 in methanol. Slides were immersed in 6% citrate buffer (pH 6) and exposed to 98 °C water bath for 40 min. Slides were primarily treated with antibody against human Ki-67 (1:40) and incubated for 1 hour at room temperature. After washing, secondary antibody Biotinylated Link (Dako) was applied (10 min at room temperature). For visualization, supersensitive one step polymer HRP (Biogenex, Fremont, California, USA) was used with AEC as chromogen. Staining without the primary antibody served as negative control. No significant background staining was detectable. The Ki-67-positive tumour cells per fields of vision were counted manually under light microscope (40-fold magnification), 5 fields of vision per tumour were evaluated. Proliferation index was calculated as percentage of Ki-67 positive cells from all cells in the field of view.

3. Results

3.1. Synthesis of VHLGYAT peptide containing daunomycin conjugates

Three daunomycin conjugates of VHLGYAT peptide amide (Dau=Aoa-VHLGYAT-NH_2, Dau=Aoa-GFLG-VHLGYAT-NH_2, Dau=Aoa-LRRY-VHLGYAT-NH_2) were prepared. Dau was attached directly to the *N*-terminus of the peptide or to a Cathepsin B cleavable spacer incorporated between the homing peptide and Dau. Two different spacers were applied (GFLG and LRRY). The peptides were built up on solid support manually using standard Fmoc/tBu strategy. The *N*-terminus of the linear peptides was modified with aminooxyacetyl moiety (Aoa) as a conjugation site. However, Aoa is very sensitive to aldehydes and ketones that results in difficulties concerning the final cleavage step and working up procedure. Therefore, Aoa was incorporated as isopropylidene protected derivative to the peptides. This protection was removed with 1 M methoxyamine under slightly acidic condition prior to the Dau conjugation (**Scheme 1**). All synthetic steps ran accordingly and the synthesis of conjugates resulted in good yields. The characteristics of the conjugates are presented in **Table 1**.

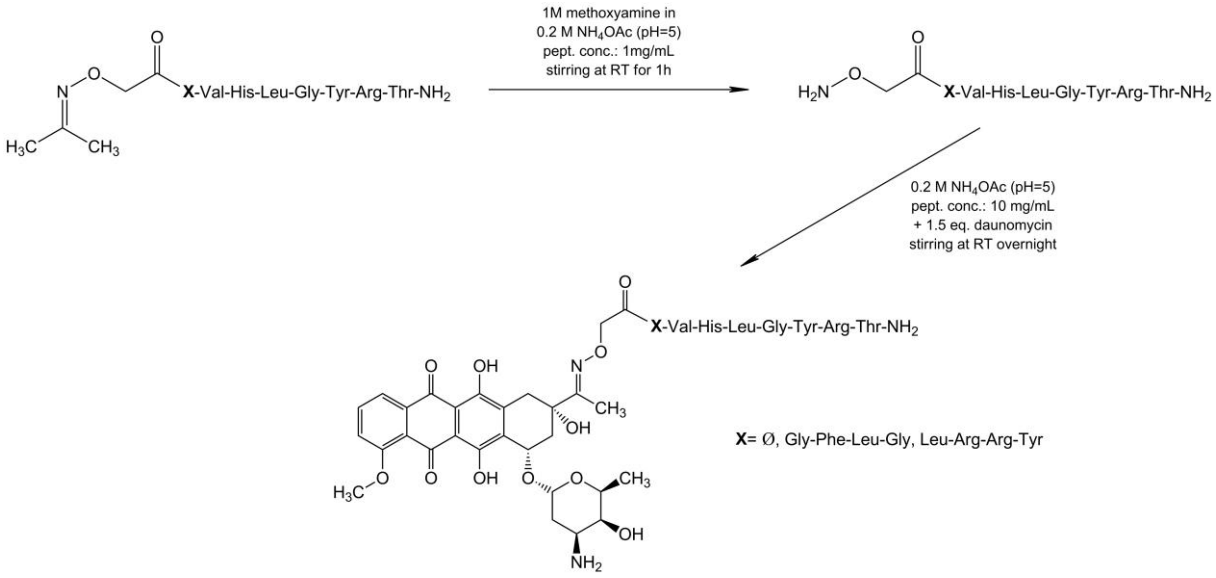

Scheme 1. Synthesis of oxime linked daunomycin – homing peptide conjugates

Table 1. Characteristics of VHLGYAT peptide containing daunomycin conjugates. RP-HPLC spectra of the conjugates can be seen in Supplementary information **S1**.

Compounds (code)	RP-HPLC R_t (min)[a]	ESI-MS calculated	ESI-MS measured[b]
Dau=Aoa-VHLGYAT-NH_2 (**1**)	26.1	1340.8	1341.0
Dau=Aoa-GFLG-VHLGYAT-NH_2 (**2**)	32.5	1715.8	1715.7
Dau=Aoa-LRRY-VHLGYAT-NH_2 (**3**)	28.2	1930.1	1929.9

[a]RP-HPLC: column: Phenomenex Aeris Peptide XB-C18 column (250 mm x 4.6 mm) with 3.6 μm; eluents: 0.1% TFA in water (A) and 0.1% TFA in acetonitrile (80:20, v/v) (B); gradient: 0 min 0% B, 5 min 0% B, 50 min 90% B; flow rate: 1 mL/min; detection: λ= 220 nm.

[b]ESI-MS: Esquire 3000+ ion trap mass spectrometer

3.2. *In vitro* cytostasis and cellular uptake of the VHLGYAT based drug conjugates

The *in vitro* cytostatic effect was measured on HT-29 human colon cancer cells. Cells were treated with the conjugates for 6 h or 24 h, then the cells were washed and incubated further. After 72 h (including the treatment period), MTT assay was used for the determination of the cytostatic effect of the conjugates. When the cells were treated with the conjugates for 6 h, only the Dau=Aoa-LRRY-VHLGYAT-NH_2 (**3**) conjugate showed moderate cytostatic effect (IC_{50} = 62.7 μM) that improved a bit during longer treatment time.

According to these results and the low solubility of conjugate **2**, we selected conjugate **3** as control conjugate for further studies (and for the subsequent assays, 24 h tretament time was used).

3.3. Synthesis of conjugates using Ala scan in the sequence of homing peptide

During the next step, all amino acids, except alanine were replaced by Ala one by one in the sequence of the homing peptide VHLGYAT. The six new conjugates were prepared as it was described above. The characteristics of the Ala scanned conjugates are summarized in **Table 2**.

Table 2. Characteristics of conjugates modified by Ala scan. RP-HPLC spectra of the conjugates can be seen in Supplementary information **S2**.

Compounds (code)	RP-HPLC R_t (min)[a]	ESI-MS calculated	ESI-MS measured[b]	IC_{50} (μM)*
Dau=Aoa-LRRY-**A**HLGYAT-NH_2 (**4**)	27.7	1901.5	1901.8	>100
Dau=Aoa-LRRY-V**A**LGYAT-NH_2 (**5**)	29.0	1863.5	1864.0	36.8±0.4
Dau=Aoa-LRRY-VH**A**GYAT-NH_2 (**6**)	27.2	1887.5	1887.8	>100
Dau=Aoa-LRRY-VHL**A**YAT-NH_2 (**7**)	28.6	1943.6	1943.9	24.1±1.6
Dau=Aoa-LRRY-VHLG**A**AT-NH_2 (**8**)	27.4	1837.5	1837.8	>100
Dau=Aoa-LRRY-VHLGYA**A**-NH_2 (**9**)	28.0	1899.8	1899.9	70.9±3.8

[a]RP-HPLC: column: Phenomenex Aeris Peptide XB-C18 column (250 mm x 4.6 mm) with 3.6 μm; eluents: 0.1% TFA in water (A) and 0.1% TFA in acetonitrile-water (80:20, v/v) (B); gradient: 0 min 0% B, 5 min 0% B, 50 min 90% B; flow rate: 1 mL/min; detection: λ= 220 nm.

[b]ESI-MS: Esquire 3000+ ion trap mass spectrometer

*Note that IC_{50} value of conjugate **3** was 46.9±9.4 μM in these experiments.

3.4. *In vitro* cytostasis and cellular uptake of conjugates using Ala scan in the sequence of homing peptide

The study of the cytostatic effect of the Ala scanned conjugates was investigated using HT-29 colon cancer cells and compared with the conjugate Dau=Aoa-LRRY-VHLGYAT-NH_2. The results indicated that the replacement of Val, Leu or Tyr to Ala (V/A (**4**), L/A (**6**), Y/A (**8**)) in the sequence of the homing peptide is not allowed without loss of cytostatic effect (IC_{50} > 100 μM). When Thr was changed to Ala (T/A (**9**)), the anti-tumour effect decreased a bit, while the modification of His (H/A (**5**)) in the sequence resulted in a slightly more active conjugate (**Table 2**). The replacement of Gly to Ala (G/A (**7**)) increased the cytostatic effect significantly (from IC_{50} = 46.9±9.4 μM to 24.1±1.6 μM) in this experiment.

The correlation between the cytostatic effect and the cellular uptake of the conjugates was investigated by flow cytometry. The percentage of the Dau positive cells (cellular uptake) and the fluorescence mean values of the cells were determined. The cells were treated with 100 μM conjugates for 3 h. About 80% of cells were Dau+ in case of G/A (**7**) conjugate which was higher than the conjugate with the parent homing peptide (*ca.* 70%). The observed difference was even more remarkable concerning fluorescence intensity values, suggesting higher cellular uptake of G/A (**7**) conjugate by cells. The other conjugates showed lower cellular uptake in the following decreasing order: T/A (**9**), V/A (**4**), H/A (**5**) (this contradicts a bit with cytostatic effect), L/A (**6**), and Y/A (**8**) (**Fig. 1**).

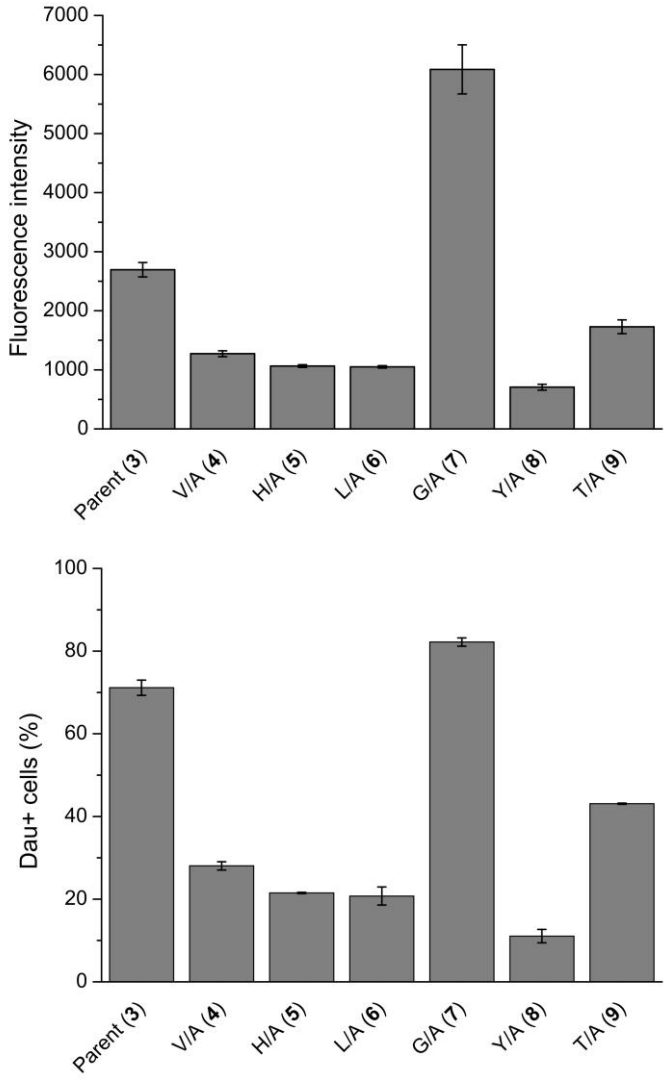

Figure 1. Cellular uptake of the conjugates prepared by Ala scan using flow cytometry and HT-29 colon cancer cells. The concentration of the drug conjugates was 100 μM. Experiments were performed in duplicates (error bars represent standard deviation).

3.5. Synthesis of conjugates using positional scanning in position 4 of the homing peptide

The results of the Ala scan indicate that the modification of position 4 has major effect on cellular uptake and cytotoxicity. Therefore, the Gly in position 4 of the homing motif was replaced by ten amino acids with different characteristics. Lys as a basic, Glu as an acidic amino acid, Thr, Ser, Tyr and Asn as polar and Phe, Cpa (*p*-chlorophenylalanine) and Leu as nonpolar (aromatic and nonaromatic) amino acids were incorporated. Furthermore, Pro that might break the conformation of the peptide was also investigated. The synthesis of the

peptides and conjugates was carried out in the same way as it was described before. The characteristics of the conjugates are summarized in **Table 3**.

Table 3. Characteristics of conjugates modified by positional scanning in position 4. RP-HPLC spectra of the conjugates can be seen in Supplementary information **S3**.

Compounds (code)	RP-HPLC R_t (min)[a]	ESI-MS calculated	ESI-MS measured[b]	IC_{50} (μM)*
Dau=Aoa-LRRY-VHL**K**YAT-NH_2 (**10**)	28.2	2000.7	2000.8	50.3±3.0
Dau=Aoa-LRRY-VHL**E**YAT-NH_2 (**11**)	29.3	2001.6	2001.7	29.5±6.3
Dau=Aoa-LRRY-VHL**L**YAT-NH_2 (**12**)	31.1	1985.7	1986.0	7.5±3.5
Dau=Aoa-LRRY-VHL**F**YAT-NH_2 (**13**)	31.2	2019.7	2019.8	6.6±2.9
Dau=Aoa-LRRY-VHL**S**YAT-NH_2 (**14**)	28.9	1959.6	1959.8	24.8±7.4
Dau=Aoa-LRRY-VHL**T**YAT-NH_2 (**15**)	29.0	1973.6	1974.0	21.7±6.5
Dau=Aoa-LRRY-VHL**N**YAT-NH_2 (**16**)	29.0	1986.6	1986.9	28.0±19.4
Dau=Aoa-LRRY-VHL**P**YAT-NH_2 (**17**)	31.2	1969.7	1970.1	>50
Dau=Aoa-LRRY-VHL**Y**YAT-NH_2 (**18**)	30.8	2035.7	2036.1	38.4±17.7
Dau=Aoa-LRRY-VHL**Cpa**YAT-NH_2 (**19**)	31.3	2053.6	2053.8	3.6±0.1

[a]RP-HPLC: column: Macherey-Nagel Nucleosil C18 column (5 μm, 100 Å; 250×4.6 mm)
eluents: 0.1% TFA in water (A) and 0.1% TFA in acetonitrile-water (80:20, v/v) (B); gradient: 0 min 0% B, 5 min 0% B, 50 min 90% B; flow rate: 1 mL/min; detection: λ= 220 nm.

[b]ESI-MS: Esquire 3000+ ion trap mass spectrometer

*Note that in these experiments, IC_{50} value of conjugates **3** and **7** were 39.4±5.9 and 27.9±6.4, respectively.

3.6. *In vitro* cytostasis and cellular uptake of conjugates using positional scanning in position 4 of the homing peptide

All conjugates, except the Pro containing one showed cytostatic effect in the measured range (**Table 3**). The incorporation of Lys in this position decreased the cytostatic effect (IC_{50} = 50.3±3.0 μM) compared to both G/A (**7**), and the native parent (**3**) conjugates (IC_{50} = 27.9±6.4 and 39.4±6.4, respectively). No significant difference in cytostatic effect was observed when the Ala was replaced by Thr (**15**), Ser (**14**), Asn (**16**) and Glu (**11**). However, it is worth to mention that the change of Ala to Ser increased the water solubility of the conjugate that might be useful in drug development. The results indicate that the incorporation of Phe (**13**) or Leu (**12**) gives the best conjugates, having 4-5 times higher cytostatic effect than the G/A (**7**) or the parent (**3**) conjugates (IC_{50} = 6.6±2.9 μM and 7.5±3.5 μM, respectively). The chlorine substitution on aromatic ring of Phe (**13**) decreased (IC_{50} = 3.6±0.1 μM), while the replacement of Phe by the more polar Tyr (**18**) increased (IC_{50} = 38.4±17.7 μM) the IC_{50} value.

We also studied the effect of the peptides without the drug (Dau) in case of (**3**) and (**13**). As a result, no effect of the peptides alone could be detected (IC_{50} > 100 μM).

Cellular uptake of the Dau-peptide conjugates (G/A (**7**), G/F (**13**), G/S (**14)**, G/P (**17**)) was studied first by confocal microscopy. Lysosomes and mitochondria were stained with specific fluorescent probes to identify the intracellular localization of the conjugates and the released metabolite.

The free Dau was taken up by cells fast and localized partly in the nucleus (**Fig. 2A**). Conjugate **13** showed a similar pattern of subcellular distribution: it exhibited a predominantly punctate pattern in cytoplasmic compartments (**Fig. 2B**). In the case of conjugate **14,** a weaker signal could be detected (**Fig. 3**). The conjugate could be detected in cytoplasmic compartments in case of living cells, however, it accumulated in the nucleus of dying cells (**Fig. 3**). Conjugate **17** exhibited an overall weaker signal than the other two derivatives (**Fig. 2C**).

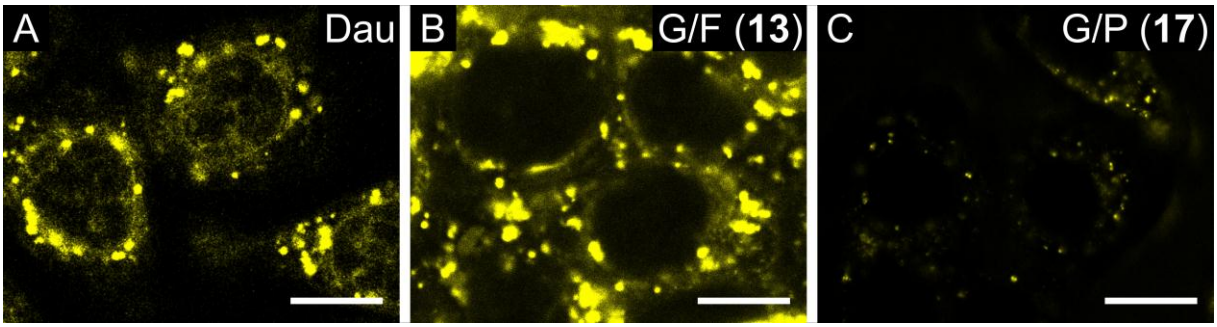

Figure 2. Cellular uptake of drug conjugates studied by confocal microscopy. (**A**, **B**, **C**) Uptake of free Dau, drug conjugates G/F (**13**) and G/P (**17**), respectively by HT-29 colon cancer cells. Cells were incubated with 50 μM Dau or drug conjugate for 90 min. The conjugates were detected at 550-600 nm (emission wavelength of daunomycin, marked by yellow). The scale bar represents 10 μm.

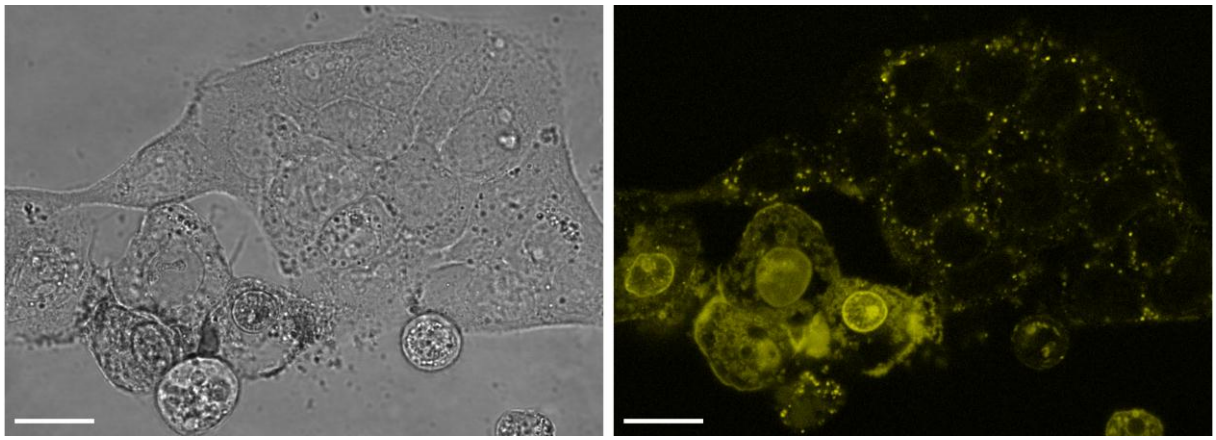

Figure 3. Comparison of phenotype of living and dead HT-29 colon cancer cells incubated with G/S (**14**) drug conjugate (incubation time: 90 min) studied by confocal microscopy. Image captured in transmitted light mode can be seen on the left. The conjugate was detected at 550-600 nm (emission wavelength of daunomycin, marked by yellow, on the right). The scale bar represents 10 μm.

Conjugate **13** was applied together with specific fluorescent dyes to follow the intracellular localization of Dau-containing derivatives. Localization of Dau-derivatives is represented in yellow, lysosome and mitochondrion specific labels with green and red, respectively. Common loci can be explored in the overlay images. The images reveal co-localization with lysosome specific fluorescent stain Lysotracker Deep Red, but not with mitochondria (**Fig. 4**).

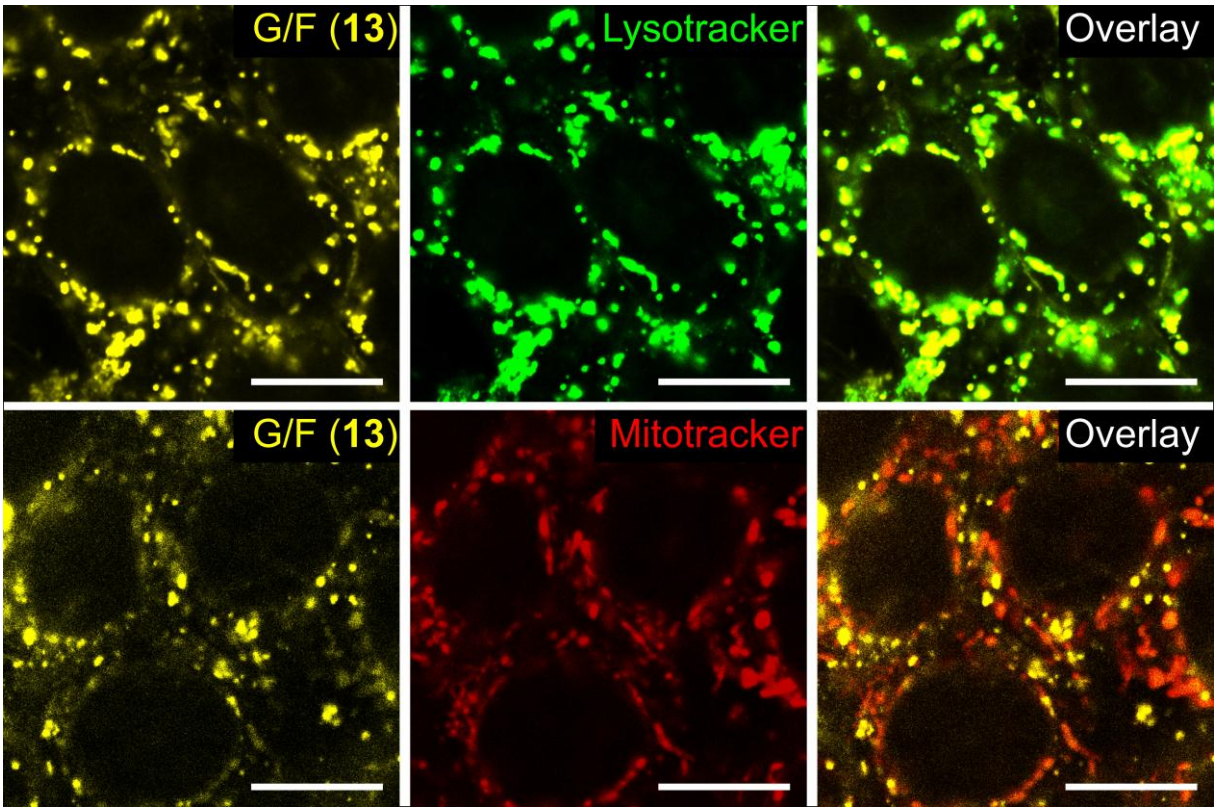

Figure 4. Study of cellular uptake of drug conjugate G/F (**13**) (yellow) by HT-29 colon cancer cells using confocal microscopy. Lysosomes were stained with Lysotracker Deep Red (upper panel, green), mitochondria were stained with MitoTracker Deep Red (lower panel, red). Cells were incubated with 50 μM drug conjugate for 30 min before imaging. The conjugate was detected at 550-600 nm (emission wavelength of daunomycin, marked by yellow). The scale bar represents 10 μm.

3.7. Synthesis of conjugates using positional scanning in position 6 of the homing peptide

The Ala in the homing peptide sequence that was not changed during Ala scanning, was replaced with different amino acids to see their influence on the biological activity. However, the starting conjugate for this was conjugate **13** containing Phe in position 4 of homing peptide. Similar to the previous positional scanning experiment Lys, Glu, Ser, Leu, Asn and Pro were incorporated to the place of Ala (**Table 4**). The synthesis and characterization were investigated as they were described above.

Table 4. Characteristics of conjugates modified by positional scanning in position 6. RP-HPLC spectra of the conjugates can be seen in Supplementary information **S4**.

Compounds (code)	RP-HPLC R_t (min)	ESI-MS calculated	ESI-MS measured	IC_{50} (μM)
Dau=Aoa-LRRY-VHL**F**Y**K**T-NH_2 (**20**)	30.5	2077.3	2077.8	11.5±1.7
Dau=Aoa-LRRY-VHL**F**Y**E**T-NH_2 (**21**)	31.9	2078.3	2078.5	54.3±13.4
Dau=Aoa-LRRY-VHL**F**Y**L**T-NH_2 (**22**)	32.3	2062.3	2062.7	3.2±0.1
Dau=Aoa-LRRY-VHL**F**Y**S**T-NH_2 (**23**)	32.1	2036.2	2036.7	17.7±2,2
Dau=Aoa-LRRY-VHL**F**Y**N**T-NH_2 (**24**)	31.8	2063.3	2063.7	15.4±6.3
Dau=Aoa-LRRY-VHL**F**Y**P**T-NH_2 (**25**)	31.6	2046.3	2046.8	10.9±0.9

[a]RP-HPLC: column: Macherey-Nagel Nucleosil C18 column (5 μm, 100 Å; 250×4.6 mm)
eluents: 0.1% TFA in water (A) and 0.1% TFA in acetonitrile-water (80:20, v/v) (B); gradient: 0 min 0% B, 5 min 0% B, 50 min 90% B; flow rate: 1 mL/min; detection: λ= 220 nm.

[b]ESI-MS: Esquire 3000+ ion trap mass spectrometer

*IC_{50} value of conjugate **13** was 6.5±0.3 in this experiment.

3.8. *In vitro* cytostasis of conjugates using positional scanning in position 6 of the homing peptide

The replacement of Ala in position 6 of the homing peptide by different amino acids had lower influence on the cytostatic effect of the conjugates (**Table 4**) except for the incorporation of Glu (**21**), that decreased the effect significantly (IC_{50} = 54.3±13.4 μM). Only

the replacement of Ala to Leu (**22**) enhanced the cytostatic effect (IC_{50} = 3.2±0.1 μM, half of that for conjugate **13**).

3.9. *In vitro* cellular uptake of conjugates using positional scanning in position 4 and 6 of the homing peptide

Four conjugates (G/F (**13**), G/S (**14**), G/P (**17**) and G/Cpa (**19**),) were selected from the group of conjugates that were modified in position 4 and one conjugate ((G/F, A/L (**22**)) was selected from the last group (scanned in position 6) for cellular uptake studies. The conjugates were compared with the parent sequence (**3**) containing and G/A (**7**) conjugates. All conjugates were applied in 6.25 μM to 100 μM concentrations. The G/F conjugate (**13**) that had one of the highest cytostatic effect entered the cells also at a lowest concentration and its uptake increased with the elevation of the concentration (**Fig. 5**). Interestingly, the cellular uptake of **13** was a bit higher than of conjugate G/Cpa (**19**) that had slightly better cytostatic effect. Significant uptake of G/A (**7**) and G/S (**14**) could be detected only at 25 μM concentration, the previous one showing higher uptake. The G/P (**17**) conjugate that did not show cytostatic effect in the measured range, could not enter the cells efficiently even at a high, 100 μM concentration. At the highest concentrations, the toxic effect of conjugate **13** and **19** was observed resulting in significantly lower number of living cells that decreased the measured fluorescence intensity. A/L change in position 6 (conjugate **22**) resulted in similar, but a bit lower cellular uptake than conjugate **13** and **19** (**Fig. 5**).

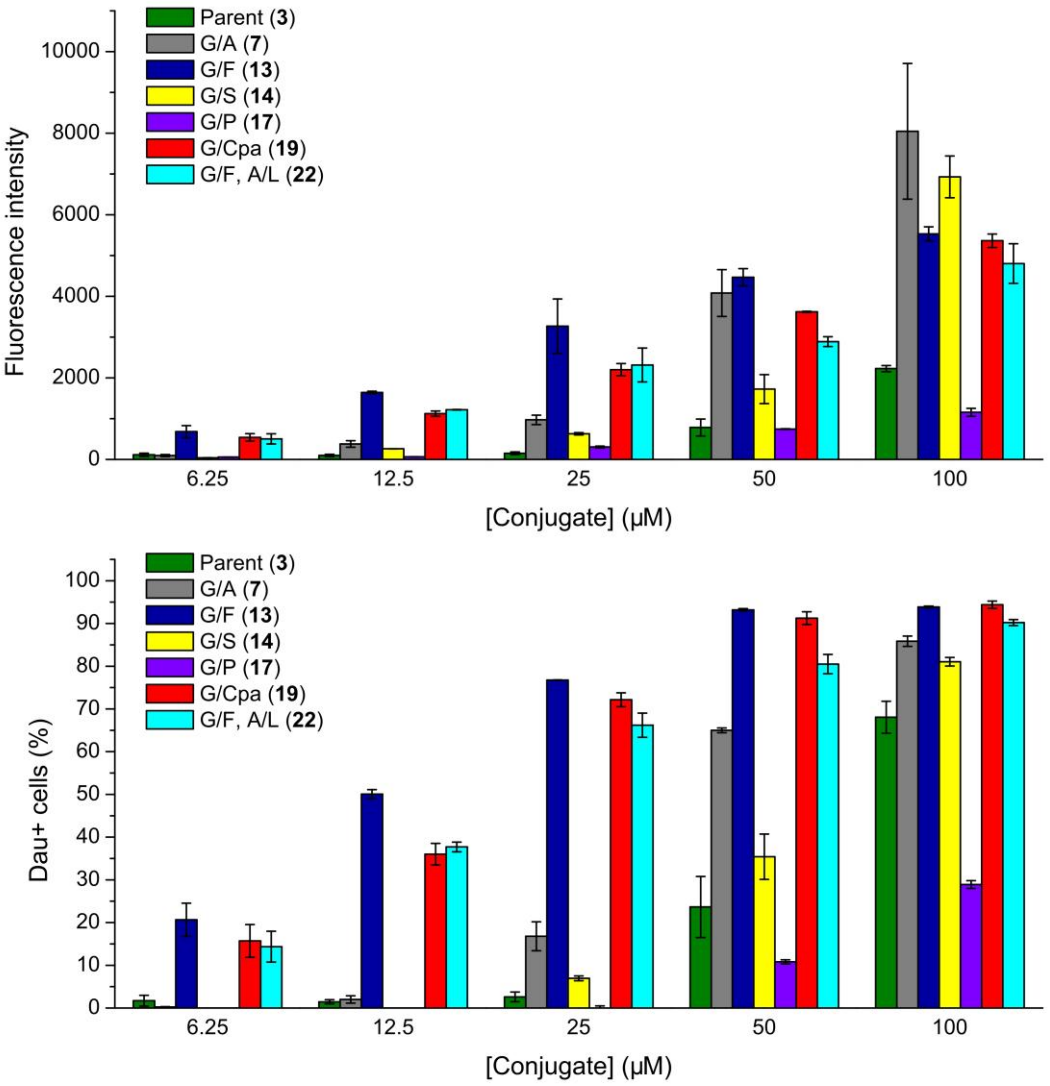

Figure 5. Comparison of the cellular uptake of drug conjugates G/F (**13**), G/S (**14**), G/P (**17**) and G/Cpa (**19**) and G/F, A/L (**22**) with parent conjugate (**3**) and G/A (**7**) using flow cytometry on HT-29 colon cancer cells. Experiments were performed in duplicates (error bars represent standard deviation).

3.10. Stability of the conjugates

The stability of selected conjugates (**3**, **7**, **13**, **14**, **17**, **19**, **22**) was studied in serum free incomplete cell culture medium at 37 °C that was applied for *in vitro* cellular uptake experiments. Samples were taken at zero time point just after the addition of the conjugates into the medium and after 3 h which is the endpoint of the cellular uptake measurements. According to the HPLC-MS spectra, none of the conjugates showed any decomposition under these circumstances (Supplementary information **S5-S11**). In addition, their stability was examined in 2.5% serum containing complete cell culture medium at 37 °C, as these

conditions were used in the *in vitro* cell viability measurements. Because 24 h treatment was applied in cell viability assays and then the conjugates were washed out from the cells, the stability experiments were continued for 24 h in this case. Samples were taken at zero time point, 3 h, 6 h and 24 h. Only parent conjugate (**3**) and the less active Pro-containing conjugate showed minor decomposition that could be detected rather at 24 h (Supplementary information **S9**). The observed cleavage point was between the two Arg in the spacer sequence resulting in Dau=Aoa-LR-OH and H-RYVHLXYAT-NH_2 (where X is Gly (**3**) or Pro (**17**). Interestingly, significant sugar loss of conjugate **17** was also detected. According to this data, we can conclude that the conjugates are stable enough (except the Pro-containing one) not to influence the *in vitro* cellular uptake and cell viability studies.

3.11. Active metabolite release from the conjugates in lysosomal homogenate

The release of the active metabolite from the parent (**3**) and the most active (**13**, **19**, **22**) conjugates was investigated in rat liver lysosomal homogenate. Very fast decomposition was observed in all cases that did not depend on the sequence of the homing peptide (**Fig. 6** and Supplementary information **S12-S14**). The main cleavage site in the spacer sequence was between the two Arg that appeared at zero time point. After 1 h Dau=Aoa-Leu-OH could be detected that increased in time while the quantity of Dau=Aoa-Leu-Arg-OH decreased. At 24 h, only the smallest Dau-containing metabolite was observed. It is worth to note that the main cleavage site in the homing peptide was between Leu-X (X is Gly or its substituted amino acid) that was identified immediately at the zero time point. Interestingly, only this cleavage site was observed in 0.2 M NaOAc solution (pH 5) as control solution, but only at 24 h (data not shown).

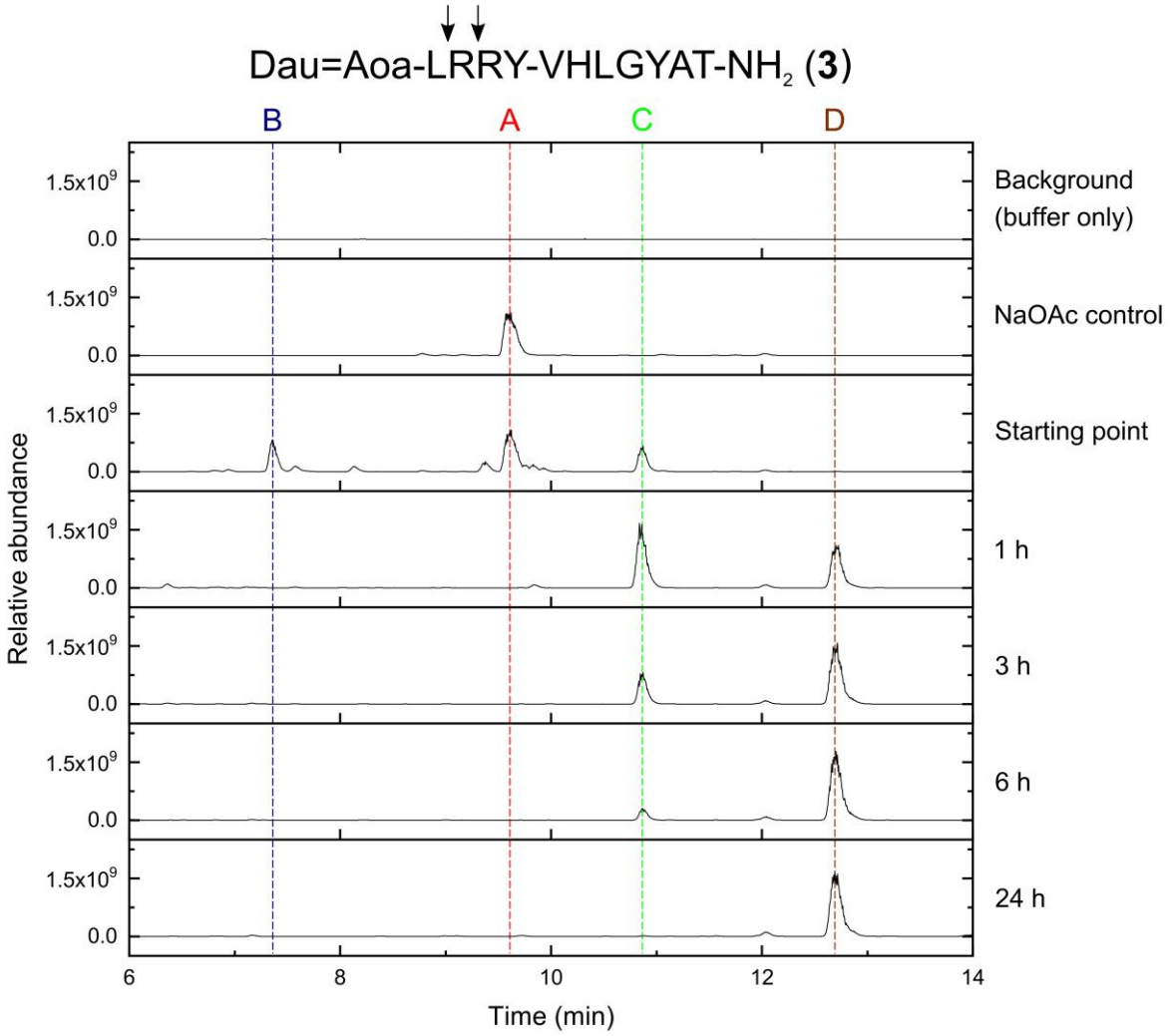

Dau=Aoa-LRRY-VHLGYAT-NH_2 (3)				
Sign	**Sequence**	**Molecular formula**	**Calculated MW**	**Measured (*m/z*)**
A	Dau=Aoa-LRRY-VHLGYAT-NH_2	$C_{91}H_{128}N_{22}O_{25}$	1928.9421	965.9786[1]
B	H-RY-VHLGYAT-NH_2	$C_{50}H_{75}N_{15}O_{12}$	1077.5720	1078.5780[2]
C	Dau=Aoa-LR-OH	$C_{41}H_{55}N_7O_{14}$	869.3807	870.3866[2]
D	Dau=Aoa-L-OH	$C_{35}H_{43}N_3O_{13}$	713.2796	714.2862[2]

Figure 6. Stability of Dau=Aoa-LRRY-VHLGYAT (**3**) in rat liver lysosomal homogenate monitored by LC-MS. Note that reaction termination in case of the "Starting point" sample took place after ~1 min. ([1] $[M+2H]^{2+}$, [2] $[M+H]^+$.)

3.12. Study of the tumour type specificity of conjugate 3 and 13

Tumour type specificity of conjugates **3** and **13** was investigated on 22 different types of tumour cell line and on MRC-5 (human fibroblast) as non-tumouricidal control cell line. The cells were treated with the compounds for 24 h followed by incubation in fresh medium for further 48 h. The IC_{50} values of the conjugates were compared to each other and to the values

received by measuring the effect of the free drug molecule (**Table 5**). The data indicate that the conjugates had cytostatic effect on all cell types, but the lowest activity was measured on MRC-5 cells. However, the conjugates were not selective to the HT-29 human colon adenocarcinoma at all. Nevertheless, conjugate **13** showed higher cytostatic effect in all cases, that was *ca.* 1.5–5 times higher activity depending on the type of cancer cells. The IC_{50} values were mainly at the low micromolar range and they were 1-2 order of magnitude higher compared to the free Dau that can enter cells by diffusion.

Table 5. Specificity study of the cytostatic effect of drug conjugates **3** and G/F (**13**) compared to free Dau on various cell lines.

Tumour type	Cell line	Dau (IC50; nM)	Conjugate 3 (IC50; µM)	Conj. 3 / Dau	Conjugate 13 (IC50; µM)	Conj. 13 / Dau	Conj. 3/ Conj. 13
Brain glioblastoma	**U-87 MG**	27.9±3.5	14.2±3.5	510.3	6.6±0.2	236.9	2.15
Breast adenocarcinoma	**MCF7**	286.0±24.7	22.2±9.2	77.6	11.1±3.8	38.8	2
Breast adenocarcinoma	**MDA-MB-231**	52.9±10.3	6.3±2.5	118.8	4.6±0.8	86.6	1.37
Mouse breast cancer	**4T1**	40.8±6.8	34.2±0.4	837.4	11.6±3.6	284.6	2.95
Colon carcinoma	**HCT 116**	127.1±21.9	33.6±4.4	264.1	7.2±0.3	57	4.67
Colon adenocarcinoma	**HT-29**	202.9 ±1.0	30.1±0.3	148.3	11.6±0.1	57.1	2.6
Colon adenocarcinoma	**WiDr**	240.1±36.3	34.1±3.2	141.8	15.1±2.9	62.8	2.26
Mouse colon carcinoma	**CT26.WT**	126.0±46.8	15.8±2.5	125.7	8.3±1.0	66	1.9
Hepatocellular carcinoma	**Hep G2**	21.3±0.9	22.4± 4.4	1052.6	4.7±0.5	220.2	4.77
Lung carcinoma	**A549**	68.2±22.7	25.9±2.3	380.1	5.9±1.5	86.1	4.39
Lung adenocarcinoma	**H1650**	47.5±1.6	4.4±1.2	92.6	2.9±0.6	60.1	1.52
Lung adenocarcinoma	**H1975**	13.3±4.7	19.3±0.1	1458.7	3.7±0.8	279.9	5.22
Melanoma	**A2058**	33.3±0.4	10.5±5.8	316.8	3.5±1.3	104.5	3
Melanoma	**M24**	93.6±25.8	15.4±3.7	164.3	5.8±0.9	61.7	2.66
Melanoma	**WM983B**	44.3±19.2	7.1±2.5	159.8	5.1±0.4	114.6	1.39
Mouse melanoma	**B16**	8.9±5.4	15.2±3.0	1711.3	3.0±0.5	335.4	5.07
Oral squamous cell carcinoma	**PE/CA PJ15**	26.7±5.0	20.2±4.6	759.3	7.4±3.4	277.3	2.73
Oral squamous cell carcinoma	**PE/CA PJ41**	25.8±5.4	9.4±3.5	363.9	4.3±0.1	165.7	2.19
Ovarian adenocarcinoma	**OVCAR-3**	472.9±63.6	13.8±0.5	29.3	11.3±2.6	24	1.22
Pancreas epithelioid carcinoma	**PANC-1**	466.7±36.6	31.7±4.5	68	26.9±8.1	57.7	1.18
Prostate carcinoma	**DU 145**	24.5±5.4	6.1±2.2	249.7	3.5±0.5	142.3	1.74
Prostate adenocarcinoma	**PC-3**	26.0±7.1	20.5±0.3	787.5	5.9±1.6	226.7	3.48
Normal fibroblast	**MRC-5**	254.7±0.6	39.3±24.6	154.2	52.1±1.7	204.6	0.75

3.13. *In vivo* tumour growth inhibition

Next to the parent conjugate **3,** one of the most active conjugate **13** was selected for *in vivo* experiments. Conjugate **13** had a bit higher solubility than conjugates **19** and **22** and no significant additional advantages of the latter ones were observed. Prior to the *in vivo* experiments, the plasma stability of the conjugates was determined in 90% human plasma. Unfortunately, the peptide – drug conjugates might adsorb to the plasma proteins, therefore, it is difficult to make an exact conclusion for plasma stability. However, the intact conjugate **13** could be still detected after 1 h by HPLC-MS while the parent conjugate **3** not (Supplementary information **S15**). The treatments were started on day 13 and the mice were terminated on day 30 after tumour transplantation, except for the free drug (Dau) group, which was terminated on day 23 after tumour transplantation due to the significant weight loss of the animals. The free drug (Dau) was administered *i.p.* using 1 mg/kg dose once a week that is the maximal tolerated dose in this case. Conjugates were injected at a dose of 10 mg/kg Dau-content three times in the first and two times in the second week. During the experiment, one animal died from both the control and Dau treated groups, while two of them from the group treated with conjugate **3**. In contrast, no animals died from the group treated with conjugate **13**. After the termination, tumour growth inhibition was calculated by the measurement of tumour weight, while liver toxicity of the compounds was determined according to the liver weight. Animal weights did not differ from control mice in case of conjugates **3** and **13**, while Dau-treated mice showed an incraesed weight loss. Animal weight data can be seen in the Supplementary information (**S16**). The results indicate that free Dau caused 84% tumour growth inhibition compared to the untreated control group (**Fig. 7A**), but it showed significant liver toxicity according to the loss of liver weight (28%). Similarly to the *in vitro* data, conjugate **13** was also more active *in vivo* in comparison with conjugate **3**. In comparison with the control group, tumour growth inhibition was significant (89%) in case of conjugate **13**, and not significant (65%) in case of conjugate **3**. Inhibition effect on tumour growth of conjugate **13**, in comparison with conjugate **3**, was on the border of significance ($p = 0.0593$). The liver mass changes were 10% and 1%, respectively, that was not significant compared to the control group, and significantly different than it was observed in case of the free Dau treated group (**Fig. 7B**).

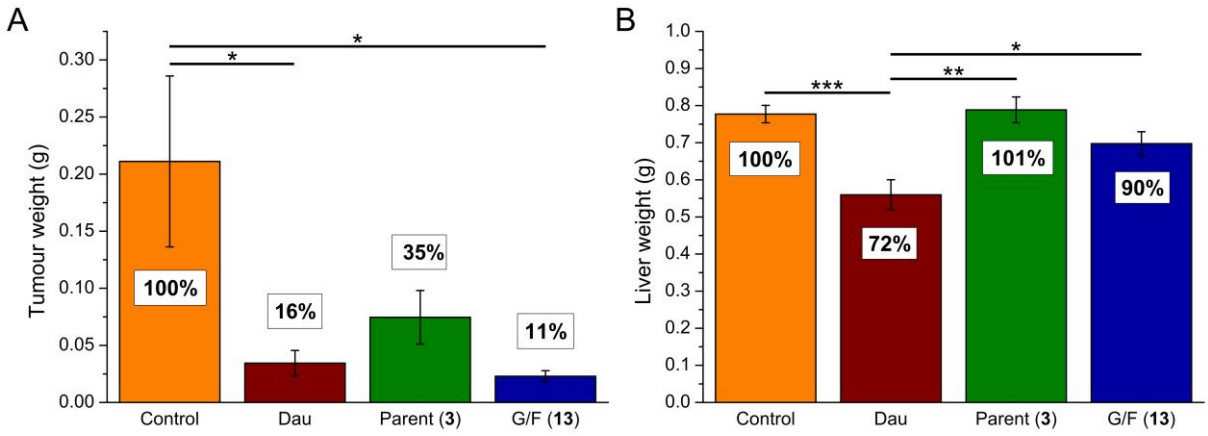

Figure 7. Comparison of tumour (**A**) and liver (**B**) weights during *in vivo* tumour growth inhibition experiment. 8-8 mice per group were treated with solvent, free Dau, drug conjugates **3** or **13** from day 13 after tumour transplantation (established by HT-29 colon cancer cells). Tumours and livers were weighed after termination of the treatments. Note that daunomycin group was terminated on day 23 after tumour transplantation due to significant weight loss of the animals. Bars represent average of weights ± standard error of mean (note that because of the death of some animals before termination, N = 7, 7, 6 and 8 from left to right). Statistical analysis was performed by Mann-Whitney test. *, ** and *** mean significant at $p<0.05$, $p<0.01$ and $p<0.001$, respectively.

To reveal the mechanism of the *in vivo* effect of conjugates and free drug (Dau), xenograft tumours were analysed by immunohistochemistry. The proportion of proliferating tumour cells was determined by Ki-67 labelling, which is a specific cellular marker for proliferation. Proliferation index was determined as % of Ki-67-positive cells per field of vision. Both conjugates significantly inhibited the number of Ki-67-positive cells in the xenograft tumour, in comparison with control tumours, where conjugate **13** inhibited at a higher degree, while free drug (Dau) did not inhibit significantly. Conjugate **13** significantly inhibited the number of Ki-67-positive cells in comparison with conjugate **3** and free drug (Dau) (**Fig. 8**).

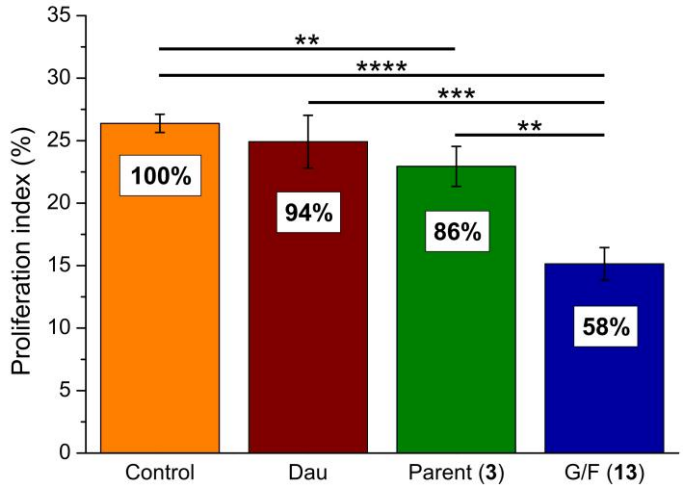

Figure 8. Comparison of the proportion of proliferating tumour cells using Ki-67 as a marker of cell proliferation. Immunodeficient SCID mice were treated with solvent (control), free Dau or drug conjugates **3** or **13** from day 13 after tumour transplantation using HT-29 colon cancer cells. After termination of the *in vivo* tumour growth inhibition experiment, tumours were fixed, embedded and stained by anti-Ki-67 antibody. Note that daunomycin group was terminated on day 23 after tumour transplantation due to significant weight loss of the animals. Proliferation index was calculated as % of Ki-67 positive cells from all cells in the field of view of the light microscope. Bars represent the average of 5 field of views of tumours of at least 3 animals per group ± standard error of mean. Statistical analysis was performed by Mann-Whitney test. *, **, *** and **** mean significant difference at $p<0.05$, $p<0.01$, $p<0.001$ and $p<0.0001$, respectively.

4. Discussion

Targeted tumour chemotherapy might be an efficient tool for cancer treatment. Development of peptide based SMDCs is a current topic in this field. In spite of the higher tissue penetration of these conjugates over ADCs, the uptake of appropriate amount of drug molecules is still questionable. Therefore, a combination of peptide based SMDCs might be necessary for effective tumour regression *in vivo*. The most effective combination might be conjugates that contain different homing peptides recognizing different cell surface compartments attached to different drug molecules with various site of action. One of the approaches to find tumour selective peptides is phage display technique. In our research, homing peptides with selectivity to HT-29 human colon adenocarcinoma were searched in the literature. According to the finding by Zhang *et al.* [13], we selected the VHLGYAT heptapeptide as homing moiety that was identified from phage library. However, we believed that the sequence could be optimized for better tumour recognition.

In the first trial, daunomycin was conjugated to the heptapeptide directly or through two different Cathepsin B cleavable linkers (GFLG or LRRY) via oxime linkage. The highest anti-tumour activity was observed in case of LRRY spacer containing conjugate that had the highest solubility as well. The results prompted us to use the LRRY spacer in our sequence modified conjugates in the further experiments. Thus, the LRRY spacer was applied for further conjugates that allows the release of the same metabolite in all cases that is important to compare the biological activity of the conjugates.

In the next step, Ala-scan was performed to identify the positions in the sequence that can be modified. Altogether, we could conclude that the Gly in position 4 of the homing motif can be modified to have better cytotoxic effect, therefore, in the further experiments this amino acid was replaced by other different amino acids (positional scanning). The results of these experiments suggested that a bulky nonpolar amino acid (Leu, Phe, Cpa) in position 4 of the homing moiety is the best choice to increase the anti-tumour activity of the conjugates developed for HT-29 colon cancer. Because Ala in position 6 of the homing peptide was not changed by Ala-scan, we wanted to check the importance of this position as well. The incorporation of different amino acids showed no significant influence on biological activity, but an apolar amino acid in this position is also preferred.

One of the key point of the biological effect of the conjugates is their efficient entry into the cells. The cellular uptake experiments indicate that the cytostatic effect and the uptake of the conjugates correlate.

The stability of some conjugates under the conditions used for the biological tests, as well as the metabolism in lysosomal homogenates were also studied. Interestingly, conjugate **3** containing the parent homing peptide decomposed faster in serum than conjugate **13** in which the Gly was replaced by Phe. In this way, not only the anti-tumour effect, but also the stability of the conjugates was also improved. The difference in the stability of the conjugates might have some influence both on the *in vitro* and *in vivo* studies. Because in all conjugates the Dau was linked to the same spacer sequence, the released metabolite in lysosomal homogenate was identical and the speed of its release was not significantly influenced by the sequence of the homing peptide. Altogether, we can conclude that the observed *in vitro* anti-tumour activity depends on the cellular uptake and the stability of the conjugates.

To measure the selectivity of the conjugates for HT-29 colon cancer cells, the anti-tumour activity of conjugate **3** with the parent homing peptide and conjugate **13** (G/F) were measured on 22 different cancer cell lines and on MRC-5 human fibroblast cells. To our surprise, both conjugates showed one of the highest IC_{50} values on HT-29 cells. Therefore, we can draw a conclusion, that the targeting moiety is not selective to HT-29 colon cancer cells. Nevertheless, conjugate **13** was more effective (1.2–5 times) than conjugate **3** on all cell lines. The lowest effect of the conjugates was observed on fibroblast cells, suggesting selectivity of the conjugates to tumour cells.

During the selection of the VHLGYAT heptapeptide by phage display, Zhang *et al*. did not identify the receptor on HT-29 cancer cells [13]. The selectivity of the peptide was not checked on a broad spectrum of tumour types either. Interestingly, our measurements on different types of cancer cell lines did not show selectivity to HT-29 cells. Therefore, we searched sequence homology in the literature. In the manuscript published by Fourie *et al.*, we found two peptides A6R (AS**HLG**L**A**R) and HbS (**VHL**TPVEK) that have overlapping sequence with our parent peptide (see in bold) [23]. Both of them bind to Hsp70 but the *de novo* A6R peptide has higher affinity. HbS peptide is originated from the *N*-terminus of hemoglobin B chain [24] and it was also indicated that hemoglobin interacts with cytosolic Hsp70 efficiently [25]. In our experiments, the replacement of Gly to Thr and Ala to Leu increases the biological effect, furthermore, these changes also enhance the similarity of the

sequence with Hbs peptide. According to the literature, heat shock protein 70 (Hsp70) is overexpressed in a large variety of different tumour types and it is localized not only intracellularly, but also tumour selective Hsp70 expression in the plasma membrane was determined [26]. A membrane Hsp70 positive tumour phenotype is associated with aggressiveness and therapy resistance of cancer and the membrane-bound Hsp70 plays a pivotal role in eliciting anti-tumour immune response. Furthermore, it can be a good target for targeted tumour therapy. All of these make a strong suggestion that VHLGYAT based homing peptides might be recognized by membrane-bound Hsp70, though further studies are in progress to confirm this assumption.

The *in vivo* tumour growth inhibition was measured on orthotopically developed HT-29 colon cancer bearing mice. The results indicate that conjugate **13** has better anti-tumour effect than conjugate **3** with the parent homing peptide. This effect was similar to the activity of the free Dau used in maximal tolerated dose, however, much lower liver toxicity was observed in the groups treated with the conjugates. In addition to the other positive quality of conjugate **13**, much lower proliferation index was obtained in tumours in the group treated with conjugate **13** than in groups treated with conjugate **3** that resulted in significantly higher tumour growth inhibition.

In conclusion, it is worth to modify tumour homing peptides selected by phage display technique for the development of small molecule drug conjugates with increased bioactivity and stability that can be applied efficiently for targeted tumour therapy. In addition, the selectivity of the conjugates has to be determined. In our case, it seems that the homing peptide selected by phage display has affinity to a broad spectrum of different tumour cells that might be related to the cell surface protein Hsp70 as possible target.

Acknowledgements

The authors would like to thank the help of Szilvia Bősze in cell biology experiments.

Funding

This work was supported by the National Research, Development and Innovation Office under grant NKFIH K119552 and NVKP_16-1-2016-0036, and by the European Union's Horizon 2020 research and innovation program under the Marie Sklodowska-Curie Grant No

642004. This research was completed in the ELTE Institutional Excellence Program (1783-3/2018/FEKUTSRAT) supported by the Hungarian Ministry of Human Capacities. These studies were also supported by grant (VEKOP-2.3.3-15-2017-00020) from the European Union and the State of Hungary, co-financed by the European Regional Development Fund.

Gitta Schlosser acknowledges the support of the MTA Premium Post-Doctorate Research Program of the Hungarian Academy of Sciences (HAS, MTA).

Conflicts of interest

The authors declare no conflict of interest.

References

1. Zhang, B., Y. Yan, Q. Shen, D. Ma, L. Huang, X. Cai, and S. Tan, A colon targeted drug delivery system based on alginate modificated graphene oxide for colorectal liver metastasis. Mater Sci Eng C Mater Biol Appl, 2017. **79**: p. 185-90. 10.1016/j.msec.2017.05.054
2. Lin, C., H.L. Ng, W. Pan, H. Chen, G. Zhang, Z. Bian, A. Lu, and Z. Yang, Exploring Different Strategies for Efficient Delivery of Colorectal Cancer Therapy. Int J Mol Sci, 2015. **16**(11): p. 26936-52. 10.3390/ijms161125995
3. Mishra, J., J. Drummond, S.H. Quazi, S.S. Karanki, J.J. Shaw, B. Chen, and N. Kumar, Prospective of colon cancer treatments and scope for combinatorial approach to enhanced cancer cell apoptosis. Crit Rev Oncol Hematol, 2013. **86**(3): p. 232-50. 10.1016/j.critrevonc.2012.09.014
4. Padma, V.V., An overview of targeted cancer therapy. Biomedicine (Taipei), 2015. **5**(4): p. 19. 10.7603/s40681-015-0019-4
5. Baudino, T.A., Targeted Cancer Therapy: The Next Generation of Cancer Treatment. Curr Drug Discov Technol, 2015. **12**(1): p. 3-20. 10.2174/1570163812666150602144310
6. Sau, S., H.O. Alsaab, S.K. Kashaw, K. Tatiparti, and A.K. Iyer, Advances in antibody-drug conjugates: A new era of targeted cancer therapy. Drug Discov Today, 2017. **22**(10): p. 1547-56. 10.1016/j.drudis.2017.05.011
7. Hagimori, M., Y. Fuchigami, and S. Kawakami, Peptide-Based Cancer-Targeted DDS and Molecular Imaging. Chem Pharm Bull (Tokyo), 2017. **65**(7): p. 618-24. 10.1248/cpb.c17-00098
8. Mezo, G. and M. Manea, Receptor-mediated tumor targeting based on peptide hormones. Expert Opin Drug Deliv, 2010. **7**(1): p. 79-96. 10.1517/17425240903418410
9. Gilad, Y., M. Firer, and G. Gellerman, Recent Innovations in Peptide Based Targeted Drug Delivery to Cancer Cells. Biomedicines, 2016. **4**(2). 10.3390/biomedicines4020011
10. Szepeshazi, K., A.V. Schally, A. Treszl, S. Seitz, and G. Halmos, Therapy of experimental hepatic cancers with cytotoxic peptide analogs targeted to receptors for luteinizing hormone-releasing hormone, somatostatin or bombesin. Anticancer Drugs, 2008. **19**(4): p. 349-58. 10.1097/CAD.0b013e3282f9adce
11. Kapoor, P., H. Singh, A. Gautam, K. Chaudhary, R. Kumar, and G.P. Raghava, TumorHoPe: a database of tumor homing peptides. PLoS One, 2012. **7**(4): p. e35187. 10.1371/journal.pone.0035187
12. Hyvonen, M. and P. Laakkonen, Identification and Characterization of Homing Peptides Using In Vivo Peptide Phage Display. Methods Mol Biol, 2015. **1324**: p. 205-22. 10.1007/978-1-4939-2806-4_14
13. Zhang, Y., J. Chen, Y. Zhang, Z. Hu, D. Hu, Y. Pan, S. Ou, G. Liu, X. Yin, J. Zhao, L. Ren, and J. Wang, Panning and identification of a colon tumor binding peptide from a phage display peptide library. J Biomol Screen, 2007. **12**(3): p. 429-35. 10.1177/1087057106299164
14. Schlage, P., G. Mezo, E. Orban, S. Bosze, and M. Manea, Anthracycline-GnRH derivative bioconjugates with different linkages: synthesis, in vitro drug release and cytostatic effect. J Control Release, 2011. **156**(2): p. 170-8. 10.1016/j.jconrel.2011.08.005
15. Hegedus, R., M. Manea, E. Orban, I. Szabo, E. Kiss, E. Sipos, G. Halmos, and G. Mezo, Enhanced cellular uptake and in vitro antitumor activity of short-chain fatty acid acylated daunorubicin-GnRH-III bioconjugates. Eur J Med Chem, 2012. **56**: p. 155-65. 10.1016/j.ejmech.2012.08.014
16. Schuster, S., B. Biri-Kovacs, B. Szeder, L. Buday, J. Gardi, Z. Szabo, G. Halmos, and G. Mezo, Enhanced In Vitro Antitumor Activity of GnRH-III-Daunorubicin Bioconjugates Influenced by Sequence Modification. Pharmaceutics, 2018. **10**(4). 10.3390/pharmaceutics10040223
17. Kapuvari, B., R. Hegedus, A. Schulcz, M. Manea, J. Tovari, A. Gacs, B. Vincze, and G. Mezo, Improved in vivo antitumor effect of a daunorubicin - GnRH-III bioconjugate modified

by apoptosis inducing agent butyric acid on colorectal carcinoma bearing mice. Invest New Drugs, 2016. **34**(4): p. 416-23. 10.1007/s10637-016-0354-7
18. Orban, E., G. Mezo, P. Schlage, G. Csik, Z. Kulic, P. Ansorge, E. Fellinger, H.M. Moller, and M. Manea, In vitro degradation and antitumor activity of oxime bond-linked daunorubicin-GnRH-III bioconjugates and DNA-binding properties of daunorubicin-amino acid metabolites. Amino Acids, 2011. **41**(2): p. 469-83. 10.1007/s00726-010-0766-1
19. Enyedi, K.N., S. Toth, G. Szakacs, and G. Mezo, NGR-peptide-drug conjugates with dual targeting properties. PLoS One, 2017. **12**(6): p. e0178632. 10.1371/journal.pone.0178632
20. Schuster, S., B. Biri-Kovacs, B. Szeder, V. Farkas, L. Buday, Z. Szabo, G. Halmos, and G. Mezo, Synthesis and in vitro biochemical evaluation of oxime bond-linked daunorubicin-GnRH-III conjugates developed for targeted drug delivery. Beilstein J Org Chem, 2018. **14**: p. 756-71. 10.3762/bjoc.14.64
21. Hegedus, R., A. Pauschert, E. Orban, I. Szabo, D. Andreu, A. Marquardt, G. Mezo, and M. Manea, Modification of daunorubicin-GnRH-III bioconjugates with oligoethylene glycol derivatives to improve solubility and bioavailability for targeted cancer chemotherapy. Biopolymers, 2015. **104**(3): p. 167-77. 10.1002/bip.22629
22. Orosz, A., S. Bosze, G. Mezo, I. Szabo, L. Herenyi, and G. Csik, Oligo- and polypeptide conjugates of cationic porphyrins: binding, cellular uptake, and cellular localization. Amino Acids, 2017. **49**(7): p. 1263-76. 10.1007/s00726-017-2428-z
23. Fourie, A.M., J.F. Sambrook, and M.J. Gething, Common and divergent peptide binding specificities of hsp70 molecular chaperones. J Biol Chem, 1994. **269**(48): p. 30470-8.
24. Braun, K.P., J.G. Pavlovich, D.R. Jones, and C.M. Peterson, Stable acetaldehyde adducts: structural characterization of acetaldehyde adducts of human hemoglobin N-terminal beta-globin chain peptides. Alcohol Clin Exp Res, 1997. **21**(1): p. 40-3. 10.1111/j.1530-0277.1997.tb03726.x
25. Basu, A. and A. Chakrabarti, Hemoglobin interacting proteins and implications of spectrin hemoglobin interaction. J Proteomics, 2015. **128**: p. 469-75. 10.1016/j.jprot.2015.06.014
26. Shevtsov, M., G. Huile, and G. Multhoff, Membrane heat shock protein 70: a theranostic target for cancer therapy. Philos Trans R Soc Lond B Biol Sci, 2018. **373**(1738). 10.1098/rstb.2016.0526